

We thank the reviewers for their insightful comments, which have allowed us to produce a stronger manuscript. Our responses to the general and specific comments are given below. Reviewer comments are provided in italics and our responses are given in plain text. Line number references pertain to the revised manuscript with no tracked changes. Quoted text from the revised manuscript is given in **blue** in this response document. We have provided revised versions of both the manuscript and the SI along with accompanying documents with changes tracked relative to the original submission.

Reviewer 1:

Reviewer 1 general comments

Wendt et al describe the design and testing of a low-cost monitor that simultaneously measures PM mass and optical depth. The manuscript is topically relevant for AMT and is generally well-written.

I have several comments below, and they generally reflect my opinion that the paper is a bit "light" and would benefit from having certain sections fleshed out in more detail. There are three figures of results (Figures 3-5), and one could argue that Figure 3 is the only one that presents truly new data. As the authors note, the AMOD is an update on the UPAS, so Figure 4 to some extent repeats the validation work for the UPAS. Likewise, several papers cited by the authors, as well as Zamora et al (DOI: 10.1021/acs.est.8b05174), have tested the Plantower sensors, so Figure 5 is not a completely novel result. My comments below reflect places where, in my opinion, the authors could add additional detail and strengthen the paper.

Response: The reviewer is correct that several studies have evaluated the performance of Plantower sensors (Levy Zamora et al. [2019], DOI: [10.1021/acs.est.8b05174](https://doi.org/10.1021/acs.est.8b05174); Bulot et al. [2019, DOI: [10.5281/zenodo.2605402](https://doi.org/10.5281/zenodo.2605402)]). The response of these light-scattering sensors to a given PM mass concentration is known to be sensitive to variations in particle size distribution, refractive index, and density. Given that these particle properties vary with time and location, the performance of these sensors is somewhat context specific. We therefore believe that, despite not being the first, our evaluation of the Plantower sensor performance (in addition to the evaluations published by other researchers) represents a valuable addition to the literature. With respect to the UPAS gravimetric sampler, prior evaluations (Volckens et al. [2017], DOI: [10.1111/ina.12318](https://doi.org/10.1111/ina.12318); Arku et al. [2018] DOI: [10.1016/j.envint.2018.02.033](https://doi.org/10.1016/j.envint.2018.02.033); Pillarisetti et al. [2019], DOI: [10.1016/j.envint.2018.11.014](https://doi.org/10.1016/j.envint.2018.11.014)) were conducted at higher concentrations, with different mechanical enclosure designs, and at varying flow rates. We therefore deemed it necessary to include additional evaluations in this manuscript.

Reviewer 1 specific comments

Major comments

1. **Comment:** *Equation 5 assumes that all of the unit-to-unit variability in the photodiodes can be quantified with one voltage, and that all units can be scaled by a single "master" unit. I think that the authors should expand on this discussion and explain how robust of an assumption this is. Even if we assume that all of the manufacturing tolerances are tight (such that manufacturing defects don't contribute to unit-to-unit variability), my overall impression is that many low-cost systems rely on components that can have high unit-to-unit variability. How safe is it to assume that all of that variability can be captured with one parameter?*

Response: We agree that many “low-cost” sensor instruments do exhibit relatively high unit-to-unit variability in their output, but we did not observe such variability with the filtered photodiodes. Thus, we are confident in the integrity of our transfer calibrations for the measurement of AOD. First, six instruments calibrated via the transfer calibration were independently validated against an AERONET monitor. These validation experiments were performed at a different AERONET site than where the original master calibration took place. Over 80% of the data points depicted in Fig. 3 were from units calibrated via the transfer calibration method. We evaluated the reliability of the transfer calibrations by comparing the performance of the master-calibrated AMOD unit with transfer-calibrated AMOD units. For measurements taken concurrently, we found negligible performance differences between the master unit and transfer-calibrated units. The average difference between transfer-calibrated units and the master unit was 0.006. All transfer-calibrated units measured AOD within 0.01 AOD units of the master unit. Five out of six transfer-calibrated units measured AOD within 0.005 AOD units of the master unit. We have added text to the sections 2.5 and 3.1 to highlight our approach and results in evaluating the transfer calibrations as provided below:

Lines 29-30 page 7 (Methods):

“Device master calibrations were conducted at the Digital Globe site and device validation tests were conducted at NEON-CVALLA.”

Lines 30-32 page 7 (Methods):

“Co-location tests took place on three separate days using seven different AMOD units: one calibrated directly relative to AERONET at the Digital Globe site, and six calibrated via the transfer calibration method (Eq. 5).”

Lines 9-12 page 9 (Results):

“We observed negligible performance differences between a master AMOD unit calibrated directly against AERONET instruments and those calibrated via transfer calibrations (Eq. 5). The average difference between units calibrated via the transfer calibration and the master unit was 0.006 AOD units.”

Second, both AERONET (Holben et al. 1998, DOI: [10.1016/S0034-4257\(98\)00031-5](https://doi.org/10.1016/S0034-4257(98)00031-5)) and GLOBE (Brooks and Mims 2001, DOI: [10.1029/2000JD900545](https://doi.org/10.1029/2000JD900545)) photometers have used transfer calibrations with a similar degree of success.

2. Comment: *The long-term robustness and/or drift of the various calibrations, or of the photodiodes themselves, is not discussed. What is a reasonable lifetime for an AMOD? What component is expected to fail first?*

Response: As the AMOD AOD sensor matures, we are gradually gaining insights into the long-term failure modes of the instrument. We expected the calibration of the AOD sensors to fail from the long-term changes of the optical interference filters, based on discussions in prior work (Brooks and Mims [2001], DOI: [10.1029/2000JD900545](https://doi.org/10.1029/2000JD900545)); Holben et al. [1998], DOI: [10.1016/S0034-4257\(98\)00031-5](https://doi.org/10.1016/S0034-4257(98)00031-5)). This turned out to be the case as we prepared for a deployment in China 12 months after the original calibrations took place. We found that two of the four units intended for deployment in China were reporting erroneous AOD data on all four channels, requiring updates to the calibration coefficients. On the remaining units, a single channel was reporting erroneous values. Based on our experience to this point, we recommend updating the AMOD AOD calibrations every six months, which is also the same period used by AERONET. We have added the following text on lines 8-9 on page 6 to state this recommendation:

“We recommend updating the calibration constants of AMOD instruments on a six-month basis to account for changes in optical properties of the filtered photodiodes used here.”

We have not yet experienced complete device failures during normal operation. All device failures have come as a result of mechanical damage during handling or calibration. While the AOD sensors do need to be re-calibrated, as stated above, we have not observed any uncorrectable failures of the components. An accurate estimate of device lifetime will require more time to allow failures to manifest.

3. Comment: *AMOD operation relies on the unit remaining still for the entire 48-hr sampling period. How can data be QC'd to make sure that the AMOD didn't move? This is discussed qualitatively on page 9 in the paragraph starting on line 5. However I think it would be much more effective if the authors could show an instance when an AMOD was operated properly and contrast that with an occasion when it was operated improperly and moved. Also, how much movement is tolerable? One can easily imagine the extreme case where someone moves the tripod. But what if the tripod shifts or shakes in the wind? How much does that impact data quality?*

Response: For large movements, the on-board accelerometer reports changes in the pitch of the AMOD relative to horizontal. We have added mention to this QC tool on lines 30-34 on page 9 as follows:

“An accelerometer reports the angular pitch of the AMOD relative to horizontal on a 30-second basis. Those data can be used to determine if the AMOD underwent large angular changes (e.g. $>2^\circ$) relative to the horizontal plane during sample collection. Wind and other disturbances can cause slight misalignment to occur between the first and second measurements that may not be detectable by the accelerometer.”

When the deviation from direct sunlight exceeds approximately 0.5° , AMOD photodiodes are no longer uniformly exposed to sunlight, leading to overpredictions of AOD. We have added the following text on lines 27-30 on page 9 to highlight this point as follows:

“The proportions of the AOD apertures permit angular deviations from direct sunlight up to approximately 0.5° for acceptable measurements. In Colorado, for example, the average day-to-day variation—for airmass values less than five—in the solar zenith and azimuth angles is 0.2° . Based on those day-to-day variations, the AMOD is most sensitive to alignment disturbances for measurements taken at the 48-hour mark.”

For angular deviations smaller than 5° , future iterations of the AMOD will feature a solar incidence angle sensor based on a quadrant photodiode. This sensor reports the incidence angle of light onto the sensor with a precision of less than 0.1° . We have included an expanded discussion of the QC potential of this sensor in the main text as follows, starting on line 33 on page 9:

“Wind and other disturbances can cause slight misalignment to occur between the first and second measurements that may not be detectable by the accelerometer. A quadrant-photodiode-based solar-alignment sensor, mounted parallel to the AOD sensors, can be used to measure solar incidence angle for deviations smaller than 5° at a precision of 0.1° . The sensor measures solar alignment based on differential signals between elements of a quadrant photodiode array.”

In our paper detailing our citizen-science deployment in Northern Colorado of ~20 AMOD’s (Discussion paper here: <https://www.atmos-meas-tech-discuss.net/amt-2019-109/>), we give multiple instances of successful AOD measurements taken over the 48-hour period by a single instrument. Small disturbances that fell within the tolerable range ($<0.5^\circ$ from direct sunlight), still allowed for successful measurements. Given the low margin of error of the instrument alignment, even minor perturbations would result in near-zero photodiode signal, which can be easily separated from successful measurements, particularly on days without cloud cover.

Here is the updated discussion on misalignment in its entirety starting at line 25 on page 9:

“AERONET co-location results indicate that the AMOD can be used to measure AOD with high accuracy when measurements are initiated and overseen by an operator; however, it remains difficult to assess the reliability of unsupervised measurements taken at 24 and 48-hour intervals after the original measurement. The proportions of the AOD apertures permit angular deviations from direct sunlight up to approximately 0.5° for acceptable measurements. In Colorado, for example, the average day-to-day variation in the solar zenith and azimuth angles is 0.2° for airmass values less than five. Based on those day-to-day variations, the AMOD is most sensitive to alignment disturbances for measurements taken at the 48-hour mark. An accelerometer reports the angular pitch of the AMOD relative to horizontal on a 30-second basis. Those data can be used to determine if the AMOD underwent large angular changes (e.g. >2°) relative to the horizontal plane during sample collection. Wind and other disturbances can cause slight misalignment to occur between the first and second measurements that may not be detectable by the accelerometer. To help catch these events, a quadrant-photodiode-based solar-alignment sensor, mounted parallel to the AOD sensors, could be added to the AMOD to measure solar incidence angle for deviations smaller than 5° at a precision of 0.1°. The sensor measures solar alignment based on differential signals between elements of a quadrant photodiode array. Without automated self-correction or operator intervention, misalignment manifests itself with erroneously high AOD measures, which are similar to cloud-contaminated measurements. Manual screening requires operator attention, which cannot be expected for a 48+ hour sampling period; however, erroneously high AOD measures, due to either misalignment or cloud contamination, can be identified and eliminated using an automated data screening algorithm.

The development of a low-cost solar tracking mount is also the subject of ongoing work. Active tracking would eliminate the need for algorithmic adjustments to account for daily solar position, enable measurement of daily AOD trends, increase solar power input, and enable robust cloud-screening algorithms. Closed-loop solar tracking will be facilitated by a quadrant diode solar-alignment sensor. Sensor-geometry specific calibration factors enable accurate computation of two-dimensional incidence angles. Incidence angle information will be used in conjunction with a closed-loop motor control algorithm to locate and track the Sun.”

As mentioned in the manuscript, AOD misalignment was one of our chief concerns with the manual version of the AMOD. Learning from the quality-control difficulties we encountered with our first deployment, we are planning to include a closed-loop motorized solar tracking feature on the next iteration of the AMOD instrument.

4. **Comment:** *Interpretation of the AMOD data seems to implicitly assume that the environment is relatively stable over the 48 hours of measurement - e.g., that PM2.5 concentrations are relatively constant and/or that hours 0, 24, and 48 have similarly sunny conditions. What*

happens if these conditions are not met? For example, what happens if there is a large change in PM_{2.5} concentration over the course of the two days? I could imagine several ways that this could happen, with potentially different impacts on the AOD/PM_{2.5} relationship. For example: (1) a photochemically active day with high secondary PM could be followed by passage of a weather front or a rain event that dramatically lowers PM_{2.5}, (2) a plume from an industrial source or a wildfire impacts the AMOD site for a portion of the sampling period. Perhaps this means that AMODs are best suited for use outside of urban areas where there are fewer sources.

Response: We have included the plantower sensor to detect changes in PM_{2.5} during the 48-hour sample. Additionally, to date, most studies of PM_{2.5} exposure and health use daily (i.e., responses to acute exposure) or annual (i.e., responses to chronic exposure) mean PM_{2.5} concentrations for exposure. “Satellite-based PM_{2.5}” estimates (e.g., van Donkelaar et al., 2006; 2010) use ~mid-day AOD from satellites to gain information on the daily mean PM_{2.5} concentrations (and these daily mean values may be averaged to annual values). These satellite-based estimates suffer from similar issues in that the AOD/PM_{2.5} relationship may change dramatically during the time of day, and mid-day conditions may not represent daily mean conditions (this is discussed in our Part 2 discussion paper: <https://www.atmos-meas-tech-discuss.net/amt-2019-109/>). Certainly sampling PM_{2.5} over two days rather than one makes these issues worse, but all of the potential issues raised by the reviewer above hold for prior satellite-based PM_{2.5} studies. With the Plantower sensor, we can investigate PM_{2.5} variability within 2-day and 1-day periods, allowing us to investigate the use of single-time AOD measurements as a proxy for time-averaged PM_{2.5} concentrations.

5. Comment: *Figure 4 shows the agreement between the AMOD and FEM PM_{2.5} measurements. Is the scatter in the data simply a reflection of uncertainty in the AMOD filter measurements? Or are there certain conditions (e.g., meteorology, PM composition on a given day) that lead to better or worse agreement?*

Response: We did not observe systematic changes in the performance of the AMOD filter measurements in response to changes in conditions. Given that these performance results are similar to those we have observed with previous iterations of our filter-based sampler, we are confident that the scatter in the data is a reflection of the uncertainty of the measurement. We also note that the FEM instrument is also subject to measurement error and imprecision, so some of the observed scatter may reflect uncertainty in the FEM filter instrument, too.

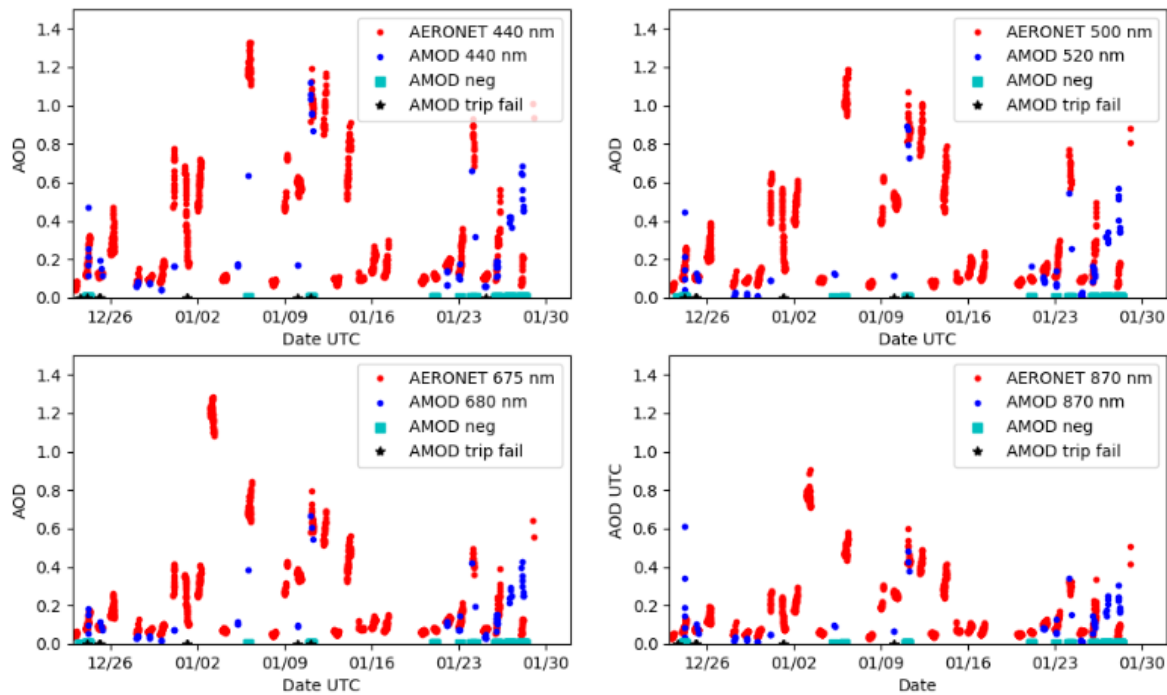
6. Comment: *How do the authors expect the AMOD to perform in a different environment? My general impression is that the Colorado Front Range is a great place to test the AMODs, since it is often sunny. I'm typing this review in a location where 24 hours ago it was sunny, today the sun is obscured by clouds and there is intermittent rain, and tomorrow will have a mix of clouds*

and sun. How well do the authors expect their sampling strategy to work in the many parts of the world where day-to-day weather, and even within-day weather, can be extremely variable?

Response: We have confidence in the ability of the AMOD PM_{2.5} filter and Plantower sensor to perform well in environments outside of typical Colorado Front Range weather. The PM_{2.5} sampler component of the AMOD has been tested at higher concentrations. Kelleher et al. (2018) (<https://doi.org/10.5194/amt-11-1087-2018>) field-tested the PM_{2.5} component at concentrations exceeding 20 $\mu\text{g m}^{-3}$. Further, the UPAS technology (the gravimetric sampling technology with which the AMOD was developed) has been evaluated against reference monitors by several groups at concentrations approaching 1000 $\mu\text{g m}^{-3}$ with similar results to reference instruments (Volckens et al. [2017] [<https://doi.org/10.1111/ina.12318>], Arku et al. [2018] [<https://doi.org/10.1016/j.envint.2018.02.033>], Pillarisetti et al. [2019] [<https://doi.org/10.1016/j.envint.2018.11.014>]). In particular, Arku et al. used the UPAS to reliably measure PM_{2.5} in 10 countries including Bangladesh, Brazil, Chile, China, Colombia, India, Pakistan, South Africa, Tanzania, and Zimbabwe. Additionally, while these studies have not shown any issue with the filter loading, the devices can be modified to run for different time durations or sample at a different rate if there are concerns about filter loading. The following text on lines 6-11 on page 11, modified slightly from the original submission for clarity and completeness, highlights this point:

“The evaluation summarized in Figure 4 was limited to relatively clean conditions in Colorado. In previous works, we have evaluated cyclone performance at concentrations from 15 $\mu\text{g m}^{-3}$ to 40 $\mu\text{g m}^{-3}$ and observed similar agreement with FEM monitors (Kelleher et al., 2018). Further, the UPAS technology (the gravimetric sampling technology with which the AMOD was developed) has been evaluated against reference monitors at concentrations approaching 1000 $\mu\text{g m}^{-3}$ and in over 10 different countries with similar results (Arku et al., 2018; Pillarisetti et al., 2019).”

The AMOD AOD sensor is less mature than its PM_{2.5} counterparts and has been evaluated, to date, under relatively limited conditions. However, we do not believe this limitation is consequential, given the high dynamic range of the photodiode light detectors used here. We also show consistent results across a fairly large AOD range during our testing under thin cirrus. In other words, we have found that these detectors are linear across several orders of magnitude of incident light intensity; thus, the sensors used in the AMOD should respond to AOD values up to ~5. Below are some example measurements from the AMOD in China showing measurements at high AOD. Note that the AERONET monitors included on the plot were not co-located with the AMODs.



With respect to weather, the AOD sensors rely upon clear skies to measure AOD correctly. This is a limitation of all AOD-sensing instruments, including those on satellites, which like the AMOD, typically measure AOD in a given location one time per day. From a mechanical and electrical weatherproofing perspective, the AMOD mechanical housing is robust to rain and snow. Therefore, the AMOD will continue sampling PM_{2.5} and attempting AOD measurements under variable weather and will measure AOD correctly when the sun is once again detectable. In locations with higher winds, we would need to consider more stable mounting options than low-cost tripods to ensure weather does not adversely affect measurements.

7. Comment: Fig 5 - Does this figure show the raw Plantower output adjusted for the filter measurements, or is some sort of humidity correction also applied?

Response: Figure 5 shows the Plantower output (with Plantower's proprietary atmospheric correction) adjusted for the filter measurement. We did not apply any humidity correction because the ambient humidity was consistently under 50% throughout the measurement period; thus, humidity artifacts are likely to be negligible for the data collected here.

Reviewer 1 minor/grammatical comments

8. Comment: In equation 3 I assume that τ (with no subscript) is the total optical depth due to aerosol, ozone, and scattering. This is not stated directly in the text. Please clarify.

Response: The reviewer is correct. This is stated in lines 18-20 on page 2 prior to the equation in the text as follows:

“By combining the aerosol, ozone absorption, and Rayleigh components into total optical depth (τ) and rearranging Eq. (2), the following equation (used for a Langley plot) is derived:”

9. **Comment:** *Page 3, Line 7: The greater than sign seems like it should come before 30.*

Response: We have corrected this mistake and lines 6-7 on page 3 now read:

“This requirement precludes the use of inexpensive photodiodes as light detectors because of their wide spectral bandpass (>30 nm).”

10. **Comment:** *Page 3, Line 30: UPAS is undefined*

Response: Thank you for pointing out this mistake. UPAS stands for Ultrasonic Personal Aerosol Sampler. We have added lines 3-5 on page 4 to define UPAS as follows:

“The AMOD design was based on a low-cost gravimetric sampler known as the Ultrasonic Personal Aerosol Sampler (UPAS), which was developed through prior work (Volckens et al., 2017).”

Response to Reviewer #2

Reviewer 2 general comments

This paper presents the development and validation of low cost sensor to measure PM mass and aerosol optical depth. The paper is interesting and within the scope of AMT. Overall paper is well written but I would recommend some minor changes in manuscript, which are listed below.

Reviewer 2 specific comments

1. **Comment:** *Introduction section is well written but I feel Line 3-11 at page 3 is a bit confusing and need to rewrite for good understanding.*

Response: We have updated the section for additional clarity as follows on lines 3-16 on page 3:

“Equation (2) assumes that the photometer measures the intensity of monochromatic light (Brooks, D. R., 2001). Because the sun emits polychromatic light, sun photometers feature light detectors with narrow spectral bandwidth (Shaw, 1983). Light detectors with full-width half-maximum (FWHM) spectral bandwidths of 15 nm or narrower can be approximated as monochromatic, permitting the application of Eq. 2 with negligible error (Brooks, D. R., 2001). The requirement of approximately monochromatic detection precludes the use of photodiode sensors with broad spectral bandpass (>30 nm). CE318 (Cimel Electronique SAS, Paris, France) sun photometers used in the Aerosol Robotics Network (AERONET), a global reference network of sun photometers, include photodiodes fitted with optical interference filters to achieve approximately monochromatic detection (Holben et al., 1998). However, high-quality bandpass filters can be cost prohibitive (e.g. >\$100) (Holben et al., 1998; Mims, 1999). The high cost of the light-sensing elements partially contributes to the overall high cost (e.g. >\$50,000) of sun photometers used in AERONET. Previous studies have used Light Emitting Diodes (LEDs) acting as detectors as a low-cost alternative to optical interference filters (Boersma and de Vroom, 2006; Brooks, D. R., 2001; Mims III, 1992). Other studies have used relatively low-cost (<\$30) integrated optical filter and photodiode modules (Murphy et al., 2016). The increasing availability of inexpensive alternatives has facilitated the production of relatively inexpensive sun photometers, which are more cost-effective for large-scale deployments (Brooks, D. R., 2001).”

2. **Comment:** *Please define what is UPAS (Line 30, page 3)?*

Response: Thank you for pointing out this mistake. UPAS stands for Ultrasonic Personal Aerosol Sampler. We have added lines 3-5 on page 4 to define UPAS as follows:

“The AMOD design was based on a low-cost gravimetric sampler known as the Ultrasonic Personal Aerosol Sampler (UPAS), which was developed through prior work (Volckens et al., 2017).”

3. **Comment:** Both Equation 5 and 6 are very important for this paper approach but there is lack of understanding in these two equations as well as overall section. I have very similar concern as Reviewer 1, which need to be addressed.

Response: We agree that many “low-cost” sensor instruments do exhibit relatively high unit-to-unit variability in their output, but we did not observe such variability with the filtered photodiodes. Thus, we are confident in the integrity of our transfer calibrations for the measurement of AOD. First, six instruments calibrated via the transfer calibration were independently validated against an AERONET monitor. These validation experiments were performed at a different AERONET site than where the original master calibration took place. Over 80% of the data points depicted in Fig. 3 were from units calibrated via the transfer calibration method. We evaluated the reliability of the transfer calibrations by comparing the performance of the master-calibrated AMOD unit with transfer-calibrated AMOD units. For measurements taken concurrently, we found negligible performance differences between the master unit and transfer-calibrated units. The average difference between transfer-calibrated units and the master unit was 0.006. All transfer-calibrated units measured AOD within 0.01 AOD units of the master unit. Five out of six transfer-calibrated units measured AOD within 0.005 AOD units of the master unit. We have added text to the sections 2.5 and 3.1 to highlight our approach and results in evaluating the transfer calibrations as provided below:

Lines 29-30 page 7 (Methods):

“Device master calibrations were conducted at the Digital Globe site and device validation tests were conducted at NEON-CVALLA.”

Lines 30-32 page 7 (Methods):

“Co-location tests took place on three separate days using seven different AMOD units: one calibrated directly relative to AERONET at the Digital Globe site, and six calibrated via the transfer calibration method (Eq. 5).”

Lines 9-12 page 9 (Results):

“We observed negligible performance differences between a master AMOD unit calibrated directly against AERONET instruments and those calibrated via transfer calibrations (Eq. 5). The average difference between units calibrated via the transfer calibration and the master unit was 0.006 AOD units.”

Second, both AERONET (Holben et al. 1998, DOI: [10.1016/S0034-4257\(98\)00031-5](https://doi.org/10.1016/S0034-4257(98)00031-5)) and GLOBE (Brooks and Mims 2001, DOI: [10.1029/2000JD900545](https://doi.org/10.1029/2000JD900545)) photometers have used transfer calibrations with a similar degree of success.

4. **Comment:** *Line 2, Page 7: Is mass flow could be changed in your setting? If yes, what would be changes in results?*

Response: Yes, our pumping hardware and software are capable of operating at different flow rates. However, we specifically designed the cyclone used for AMOD validation testing and our early deployments for operation at 2 L min^{-1} . If the flow rate was configured differently without replacing the cyclone, the collected sample would not accurately represent the ambient $\text{PM}_{2.5}$ concentration: lower flow rates would cause undersampling errors and higher flow rates would cause oversampling errors. We designed the AMOD housing, the cyclone body, and the AMOD-cyclone mechanical interface such that cyclones can easily be replaced for different flow rate selections. For example, in phase two of our citizen-science deployment, we plan to run the sampler at 1 L min^{-1} , using a specially designed cyclone and appropriately modified configuration software. We have already conducted multiple successful field tests at 1 L min^{-1} with multiple AMOD units.

5. **Comment:** *Line 12-13, Page 7: Here need to give some detail of measurements of AMOD taken by citizen scientists.*

Response: We have submitted this manuscript as part 1 of a two-part work. Part 1 details the device design and validation, and Part 2 details the results from our citizen science pilot campaign in Northern Colorado. Here is a link to the AMT discussion paper for Part 2 of our work: <https://www.atmos-meas-tech-discuss.net/amt-2019-109/>.

6. **Comment:** *Section 2.5: Please provide proper description of references instruments.*

Response: We have added additional detail to the descriptions of the AOD and real-time $\text{PM}_{2.5}$ reference monitors. The modified paragraph for AOD testing starting on line 23 on page 7 as follows:

“AMOD AOD measurements were validated in a series of co-location studies using AERONET CE318 monitors as the reference method (Holben et al., 1998). CE318 monitors used in the co-location studies had a 1.2° full angle field of view and measured AOD at eight wavelengths: 340 nm, 380 nm, 440 nm, 500 nm, 675 nm, 870 nm, 1020 nm, and 1640 nm (Holben et al., 1998). The CE318 monitors used stepping motors and closed loop control to locate and track the sun and reported measurements every 3-15 minutes when solar alignment was achieved (Holben et al., 1998). AERONET monitors were available at two sites along the Colorado Front Range:

NEON-CVALLA (N 40°09'39", W 105°10'01") and Digital Globe (N 40°08'20", W 105°08'13"). Device master calibrations were conducted at the Digital Globe site and device validation tests were conducted at NEON-CVALLA. Co-location tests took place on three separate days using seven different AMOD units: one calibrated directly relative to AERONET at the Digital Globe site, and six calibrated via the transfer calibration method (Eq. 5). Between two and four calibrated AMOD units were randomly selected on each testing day and deployed within 50 m of the AERONET monitor. Four-wavelength AMOD AOD measurements were taken at five-minute intervals over the course of one to four hours on each measurement day. AMOD data were then compared with Level 1.0 AOD data published in the online AERONET database (Holben et al., 1998). AMOD measurements concurrent within 2 minutes of an AERONET measurement were included in the comparison data set for the wavelength in question. The 500 nm and 675 nm AOD values from the AERONET instruments were adjusted—using Eq. (4) and Ångström coefficients from the AERONET data set—to match the 520 nm and 680 nm channels on the AMOD, respectively. The 440 nm and 870 nm channels required no adjustment because the AMOD and the AERONET monitors both measure at those wavelengths."

The modified paragraph for real-time PM_{2.5} testing on lines 18-26 on page 8 is provided below:

"The PM_{2.5} mass concentrations measured using the PMS5003 included in the AMOD were evaluated against a co-located light-scattering FEM monitor (GRIMM EDM 180, Ainring, Germany) at the Colorado State University main campus (EPA monitoring site 08-069-0009). The GRIMM utilized a 660 nm diode laser cell couple with a light detector to measure particle concentrations based on light scattering. Flow through the GRIMM was maintained at 1.2 L min⁻¹. PM_{2.5} readings from the AMOD PMS5003 were corrected *post hoc*, relative to the AMOD filter, by multiplying each light-scattering reading by a scaling factor equal to the ratio of the filter measurement to the 48-hr average of the PMS5003. The PMS5003 outputs uncorrected PM-_{2.5} concentrations as well as PM--_{2.5} concentrations with a proprietary correction factor for use under atmospheric conditions. We used the corrected data output by the PMS5003 for our analyses. Hourly averages of the corrected readings were then calculated for comparison to the hourly concentrations reported by the GRIMM EDM 180."

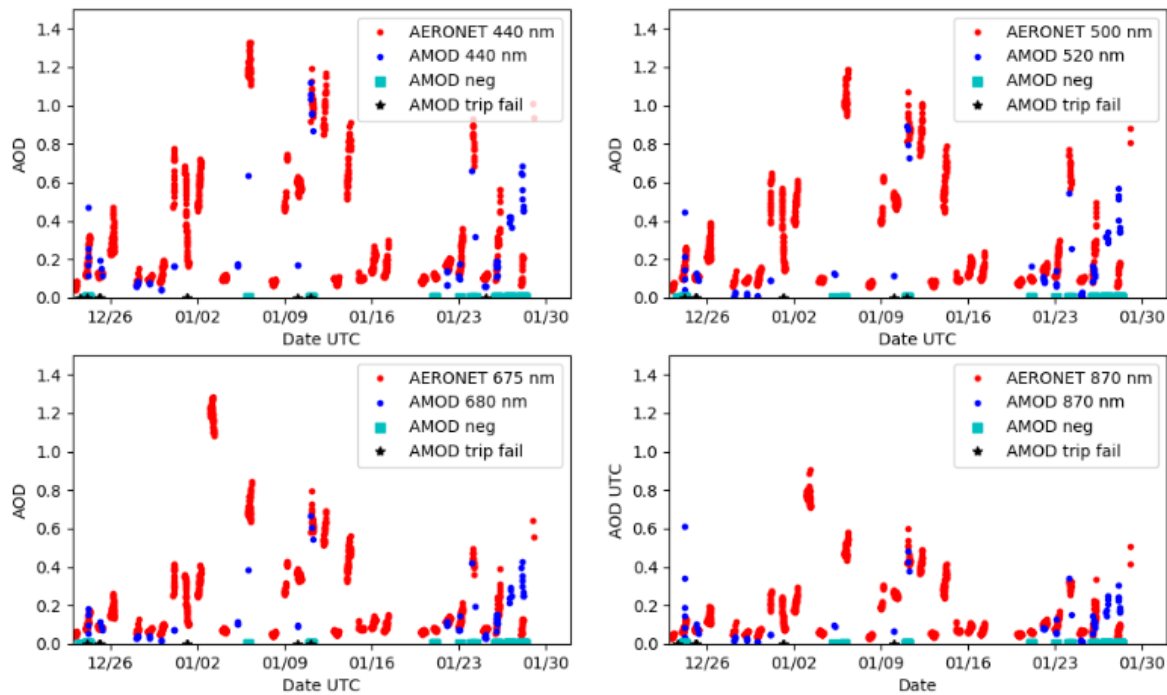
7. Comment: *What is the explanation of performance of AMOD in different atmospheric conditions i.e. rainy, clear sky, high humidity and very low temperature conditions. Assumptions and restrictions of these conditions should be added in the manuscript.*

Response: We have confidence in the ability of the AMOD PM_{2.5} filter and Plantower sensor to perform well in environments outside of typical Colorado Front Range weather. The PM_{2.5} sampler component of the AMOD has been tested at higher concentrations. Kelleher et al. (2018) (<https://doi.org/10.5194/amt-11-1087-2018>) field-tested the PM_{2.5} component at concentrations

exceeding $20 \mu\text{g m}^{-3}$. Further, the UPAS technology (the gravimetric sampling technology with which the AMOD was developed) has been evaluated against reference monitors by several groups at concentrations approaching $1000 \mu\text{g m}^{-3}$ with similar results to reference instruments (Volckens et al. [2017] [<https://doi.org/10.1111/ina.12318>], Arku et al. [2018] [<https://doi.org/10.1016/j.envint.2018.02.033>], Pillarisetti et al. [2019] [<https://doi.org/10.1016/j.envint.2018.11.014>]). In particular, Arku et al. used the UPAS to reliably measure PM_{2.5} in 10 countries including Bangladesh, Brazil, Chile, China, Colombia, India, Pakistan, South Africa, Tanzania, and Zimbabwe. Additionally, while these studies have not shown any issue with the filter loading, the devices can be modified to run for different time durations or sample at a different rate if there are concerns about filter loading. The following text on lines 6-11 on page 11, modified slightly from the original submission for clarity and completeness, highlights this point:

“The evaluation summarized in Figure 4 was limited to relatively clean conditions in Colorado. In previous works, we have evaluated cyclone performance at concentrations from $15 \mu\text{g m}^{-3}$ to $40 \mu\text{g m}^{-3}$ and observed similar agreement with FEM monitors (Kelleher et al., 2018). Further, the UPAS technology (the gravimetric sampling technology with which the AMOD was developed) has been evaluated against reference monitors at concentrations approaching $1000 \mu\text{g m}^{-3}$ and in over 10 different countries with similar results (Arku et al., 2018; Pillarisetti et al., 2019).”

The AMOD AOD sensor is less mature than its PM_{2.5} counterparts and has been evaluated, to date, under relatively limited conditions. However, we do not believe this limitation is consequential, given the high dynamic range of the photodiode light detectors used here. We also show consistent results across a fairly large AOD range during our testing under thin cirrus. In other words, we have found that these detectors are linear across several orders of magnitude of incident light intensity; thus, the sensors used in the AMOD should respond to AOD values up to ~5. Below are some example measurements from the AMOD in China showing measurements at high AOD. Note that the AERONET monitors included on the plot were not co-located with the AMODs.



With respect to weather, the AOD sensors rely upon clear skies to measure AOD correctly. This is a limitation of all AOD-sensing instruments, including those on satellites, which like the AMOD, typically measure AOD in a given location one time per day. From a mechanical and electrical weatherproofing perspective, the AMOD mechanical housing is robust to rain and snow. Therefore, the AMOD will continue sampling PM_{2.5} and attempting AOD measurements under variable weather and will measure AOD correctly when the sun is once again detectable. In locations with higher winds, we would need to consider more stable mounting options than low-cost tripods to ensure weather does not adversely affect measurements.

8. Comment: *I request to add a conclusions section along with scope recommendations.*

Response: We have added a conclusion and scope recommendations section on lines 22-29 on page 12 as follows:

“The AMOD is a lightweight and compact alternative to the instruments typically used to sample AOD and PM_{2.5}. The AMOD represents a substantial cost saving compared with alternative AOD and PM_{2.5} mass concentration sampling equipment. In field testing, the AMOD exhibit agreement within 10% when compared with AOD and PM_{2.5} reference instruments. The AMOD has been validated only in a relatively clean air in Colorado in fall and wintertime; more validation in other environments of varying pollution/weather patterns is needed. The small size, durability, increased sampling capabilities and relatively low cost of the AMOD make it a viable option for large scale and spatially dense deployments. Such data sets have the potential to

facilitate the calibration and validation of satellite-based sensors as they progress toward higher spatial resolution measurement capabilities.”

Below is the text specifically related to scope recommendations on lines 25-26 on page 12:

“The AMOD has been validated only in a relatively clean airshed in Colorado in wintertime; more validation in other environments of varying pollution/weather patterns is needed.”

~~A Low-Cost Monitor for Simultaneous Measurement of Fine Particulate Matter and Aerosol Optical Depth~~

A low-cost monitor for simultaneous measurement of fine particulate matter and aerosol optical depth. Part 1: Specifications and testing

5 Eric A. Wendt¹, Casey W. Quinn², Daniel D. Miller-Lionberg³, Jessica Tryner¹, Christian L'Orange¹,
Bonne Ford⁴, Azer P. Yalin¹, ~~Jeffery~~ Jeffrey R. Pierce⁴, Shantanu Jathar¹, and John Volckens^{1,2}

¹Department of Mechanical Engineering, Colorado State University, Fort Collins, 80523, USA

²Department of Environmental and Radiological Health Sciences, Colorado State University, Fort Collins, 80523, USA

³Access Sensor Technologies, LLC, Fort Collins, USA, 80523, USA

10 ⁴ Department of Atmospheric Science, Colorado State University, Fort Collins, 80523, USA

Correspondence to: John Volckens (john.volckens@colostate.edu)

Abstract. Globally, fine particulate matter (PM_{2.5}) air pollution is a leading contributor to death, disease, and environmental degradation. Satellite-based measurements of aerosol optical depth (AOD) are used to estimate PM_{2.5} concentrations across

15 the world, but the relationship between satellite-estimated AOD and ground-level PM_{2.5} is uncertain. Sun photometers measure AOD from the Earth's surface and are often used to improve satellite data; however, reference-grade photometers and PM_{2.5} monitors are expensive and rarely co-located. This work presents the development and validation of the Aerosol Mass and Optical Depth (AMOD) sampler, an inexpensive and compact device that simultaneously measures PM_{2.5} mass and AOD. The AMOD utilizes a low-cost light-scattering sensor in combination with a gravimetric filter measurement to quantify ground-
20 level PM_{2.5}. Aerosol optical depth is measured using optically filtered photodiodes at four discrete wavelengths. Field validation studies revealed agreement within 10% for AOD values measured between co-located AMOD and AErosol RObotics NETwork (AERONET) monitors and for PM_{2.5} mass measured between co-located AMOD and EPA Federal Equivalent Method (FEM) monitors. These results demonstrate that the AMOD can quantify AOD and PM_{2.5} accurately at a fraction of the cost of existing reference monitors.

25 1 Introduction

Fine particulate matter air pollution (PM_{2.5}) is a leading contributor to premature death and disease globally (Brauer et al., 2016; Forouzanfar et al., 2016). When inhaled, PM_{2.5} can penetrate deep into the lungs, which can cause long- and short-term health problems (Nel, 2005; Pope and Dockery, 2006). In 2015, approximately 4.2 million premature deaths were attributed to ambient PM_{2.5} exposure (Forouzanfar et al., 2016).

Recently, satellite observations have been used to estimate PM_{2.5} levels at the Earth's surface. These estimates have facilitated global estimates air pollution's impact on public health, especially in remote and resource-limited environments (Brauer et al., 2016). Satellite-based observations provide an estimate of aerosol optical depth (AOD), a dimensionless measure of light extinction in the atmospheric column. Satellite-derived AOD retrievals are then used to estimate PM_{2.5} concentrations 5 at the Earth's surface (van Donkelaar et al., 2006, 2010; Lv et al., 2016). The relationships between AOD and PM_{2.5} concentration, has been expressed as follows (Snider et al., 2015):

$$PM_{2.5} = \eta \cdot AOD \quad (1)$$

where η is a conversion factor between PM_{2.5} and AOD. If η is known, satellite AOD estimates can be directly converted to surface PM_{2.5} concentrations. However, this conversion factor is sensitive to aerosol properties, aerosol composition, surface 10 reflectivity, and vertical profile, all of which can vary across time and space (van Donkelaar et al., 2006, 2010, 2013). Thus, satellite estimates of AOD are prone to error (Boersma and de Vroom, 2006; Brooks, D. R., 2001; Holben et al., 1998; Mims, 1999; Snider et al., 2015).

To improve satellite AOD retrievals, sun photometers are routinely used to measure AOD from the Earth's surface (Levy et al., 2005). Sun photometers use photodetectors to measure the incident flux of photons at a given wavelength of light. 15 In conjunction with the Beer-Lambert-Bouger law, aerosol optical depth (τ_a) may be calculated from a Sun photometer measurement per the following equation:

$$\tau_a(\lambda) = \frac{1}{m} \left(\ln \left(\frac{V_0}{R^2} \right) - \ln(V) \right) - \tau_R(\lambda, p) - \tau_{O3} \quad (2)$$

where, m is the relative optical air mass factor, which accounts for different path lengths through the atmosphere when the sun is at different angles, R is the Earth-sun distance in astronomical units (AU), V is the voltage read by the light detector, τ_R 20 accounts for Rayleigh scattering by air molecules, p is the pressure, λ is the wavelength, τ_{O3} accounts for ozone absorption, and the extraterrestrial constant, V_0 , is the voltage produced by incident light at the top of the atmosphere (Brooks, D. R., 2001; Vroom and Amsterdam, 2003). V_0 must be evaluated via calibration. The primary method to find V_0 is the Langley plot method (Rollin, 2000). By combining the aerosol, ozone absorption, and Rayleigh components into total optical depth (τ) and rearranging Eq. (2), the following equation (used for a Langley plot) is derived:

$$25 \quad \ln(V) = \ln \frac{V_0}{R^2} - \tau \cdot m \quad (3)$$

During a Langley calibration, voltage measurements are taken as the air mass factor changes over the course of a day. The slope of the line gives total optical depth and the intercept at $m = 0$ gives the constant V_0 . Secondary extraterrestrial constant calibrations may be performed relative to units calibrated via the Langely plot method (Boersma and de Vroom, 2006). Relative calibrations may be performed by taking coincident measurements with a calibrated and an uncalibrated unit and solving Eq. 30 (2) for V_0 , with V equal to the light detector voltage from the uncalibrated unit, τ_a equal to the AOD reported by the calibrated unit, and all other parameters equal to those reported by the uncalibrated unit.

When AOD is measured at multiple wavelengths, and the Ångström exponent, α , is known, AOD for non-measured wavelengths may be inferred from the following relation (Ångström, 1929):

$$\tau_a(\lambda) = \tau_{a0} \cdot (\lambda_0) \cdot \left(\frac{\lambda}{\lambda_0}\right)^{-\alpha} \quad (4)$$

where λ_0 is a wavelength measured by the photometer, λ is the new wavelength and τ_{a0} is the measured AOD from the photometer. The Ångström exponent varies depending on the aerosol size distribution; α tends to decrease with increasing particle size and may not be constant across all wavelength pairs (Eck et al., 1999; O'Neill, 2003). When AOD is measured at 5 multiple wavelengths, curvature in α can be calculated, providing more insight into the aerosol properties (Eck et al., 1999).

Equation (2) assumes that the photometer measures the intensity of monochromatic ~~incident~~ light (Brooks, D. R., 2001). Because the sun ~~is a~~ emits polychromatic ~~emitter~~ light, sun photometers feature light detectors ~~of~~ with narrow spectral bandwidth (Shaw, 1983). Light detectors with full-width half-maximum (FWHM) spectral bandwidths of 15 nm or narrower can be approximated as monochromatic, ~~permitting the application of Eq. 2 with negligible error~~ (Brooks, D. R., 2001).

10 ~~This~~^{The} requirement ~~of approximately monochromatic detection~~ precludes the use of ~~inexpensive photodiodes as light detectors because of their wide photodiode sensors with broad spectral bandpass (>30 nm)~~. ~~The~~ CE318 (Cimel Electronique SAS, Paris, France) ~~sun photometers~~ used in the Aerosol Robotics Network (AERONET), ~~a global reference network of sun photometers~~, include photodiodes fitted with optical interference filters to achieve ~~approximately~~ monochromatic detection (Holben et al., 1998). However, high-quality bandpass filters can be cost prohibitive ~~(e.g. >\$100)~~ (Holben et al., 1998; Mims, 15 ~~1999). High cost (e.g., >\$50,000) and maintenance requirements have disqualified the use of expensive interference filter sun photometers in large scale validation studies and in locations where adequate capital and line power are lacking. The high cost of the light-sensing elements partially contributes to the overall high cost (e.g. >\$50,000) of sun photometers used in AERONET. Previous studies have used Light Emitting Diodes (LEDs) acting as detectors as a low-cost alternative to optical interference filters (Boersma and de Vroom, 2006; Brooks, D. R., 2001; Mims III, 1992). Other studies have used relatively 20 low-cost (<\$30) integrated optical filter and photodiode modules (Murphy et al., 2016). The increasing availability of inexpensive alternatives has facilitated the production of relatively inexpensive sun photometers, which are more cost-effective for large-scale deployments (Brooks, D. R., 2001).~~

PM_{2.5} samplers co-located with sun photometers can help inform the relationship between AOD and surface PM_{2.5} concentration. The U.S. Environmental Protection Agency, which regulates ambient concentrations of PM_{2.5} mass (Noble et 25 al., 2001), has designated a list of Federal Reference Methods (FRMs) and Federal Equivalent Methods (FEMs) that are used to monitor PM_{2.5} (US EPA, 2017) according to a set of design and performance characteristics (Noble et al., 2001). Like reference-grade sun photometers, the deployment prospects of FRM and FEM monitors are limited by their cost (\$10,000-\$30,000) and the need for line power.

30 The objective of this work was to develop a user-friendly and low-cost (relative to reference methods) aerosol sampler capable of accurate and precise AOD and PM_{2.5} measurements. We combined filtered-photodiode-based AOD measurements, time-resolved PM_{2.5} measurement via light-scattering, and a time-integrated, gravimetric PM_{2.5} mass measurement to accomplish this objective. The resultant device, the Aerosol Mass and Optical Depth (AMOD) sampler, is capable of simultaneous sun photometry and mass-based particulate matter measurements. In this work, we describe the design of the

first-generation AMOD and its validation against reference monitors in real-world environments. We conclude this work by evaluating the shortcomings of this generation of the AMOD and specifying ongoing design improvements.

2. Materials and Methods

2.1 Instrument Design

5 The AMOD design was based on a low-cost gravimetric sampler known as the Ultrasonic Personal Aerosol Sampler (UPAS), which was developed through prior work (Volckens et al., 2017). The original, wearable UPAS housing was designed to measure personal exposure to aerosols in indoor and work environments (Volckens et al., 2017). Later, UPAS technology was integrated into a weatherproof housing for outdoor deployments to sample wildland fire smoke (Kelleher et al., 2018). The scientific goals of the AMOD development dictated the UPAS be modified for outdoor and primarily stationary 10 measurement of both PM_{2.5} and AOD. Notable modifications included: a) additional hardware to support AOD measurement capability; b) firmware updates for simultaneous PM_{2.5} and AOD sampling; c) inclusion of a low-cost light-scattering sensor for real-time PM_{2.5} measurement; d) a larger battery and a solar panel for extended battery life; and e) a new weather-resistant housing. A computer-aided rendering highlighting key internal and structural components of the AMOD is provided in Figure 1.

15 The design of the AOD measurement system began with the selection of light sensors. Candidate sensors included filtered photodiodes (Murphy et al., 2016), (Intor Inc., Socorro, NM, USA), ~~light emitting diodes~~ (LEDs; Lighthouse LED A-FSMUBC12, WA, USA) (Mims III, 1992), and vertical cavity surface emitting lasers (VCSELs; Vixar Inc. I0-0680M-0000-KP01, Plymouth, MN, USA) – the latter two operated as detectors (Guenter and Tatum, 2002). These sensor options were evaluated according to cost, variety of available center wavelengths, and spectral bandpass measured at full-width half- 20 maximum (FWHM). Spectral bandpass measurements were made using a tunable light source (Optometrics TLS-25M, Littleton, MA, USA) for LED detectors and a tunable dye laser (Sirah Lasertechnik Allegro, Grevenbroich, Germany) for filtered photodiode and VCSEL detectors (Figure S1). Filtered photodiodes were selected for use in the AMOD due to their sufficiently narrow spectral response bandwidth (<15 nm) and relatively low cost. Filtered photodiodes were also commercially available at center wavelengths from 400 nm to 1000 nm in increments of approximately 10 nm. No other detector option offered ~~assuch a~~ a broad of a selection of wavelengths. LEDs were the least expensive option but were not selected due to their broad spectral response bandwidth. VCSELs were cost prohibitive and exhibited multiple undesirable response peaks (Figure 25 S1).

A printed circuit board containing AOD measurement instrumentation was designed using Autodesk® EAGLE. When populated, this board contained four filtered photodiodes (Figure S2), a quad operational amplifier with low leakage current 30 (Linear Technology LTC 6242, Milpitas, California, USA) and a 16-bit analog-to-digital converter (Texas Instruments ADS1115, Dallas, Texas, USA). Photodiode wavelengths of 440 nm, 520 nm, 680 nm, and 870 nm were selected to avoid molecular absorption bands, to match wavelengths used by AERONET, and to facilitate aerosol size evaluation (O'Neill,

2003). The board included a solar incidence sensor (Solar MEMS NANO-ISS5, Seville, Spain) and a Wi-Fi module (Espressif Systems ESP8266, Shanghai, China). A GPS (u-blox CAM-M8, Thalwil, Switzerland) provided location data (longitude, latitude, and altitude) needed to calculate the position of the Sun and estimate ozone optical depth. The board included circuitry for two optional components: 1) a solar incidence sensor (Solar MEMS NANO-ISS5, Seville, Spain), and 2) a Wi-Fi module (Espressif Systems ESP8266, Shanghai, China). The AOD measurement board was interfaced with the primary UPAS motherboard via I2C and UART communication. Sampler control firmware was written in C++ on the mbedTM platform (ARM[®] Ltd., Cambridge, UK).

5 A light-scattering particulate-matter sensor (Plantower PMS5003, Beijing, China) was integrated into the sampler housing (Figure 1). The PMS5003 included a fan that pulled aerosol through the path of a laser diode and a photodetector.

10 Particulate matter concentrations were evaluated by a microprocessor embedded in the PMS5003 and accessed via serial communication (Zhou Yong, 2016). Performance of Plantower light scattering sensors has been described previously (AQ-SPEC, n.d.; Kelly et al., 2017). Performance of Plantower light scattering sensors has been described previously (Bulot et al., 2019; Levy Zamora et al., 2019).

15 The AMOD housing was designed using SolidWorks[®] (ANSYS, Inc., Canonsburg, PA, USA) and built using stereolithographic printing. The housing included four tubes that limited the field of view of the light detectors. Light entered through 5-mm diameter apertures on the top surface of the housing and subsequently passed through 112 mm long tubes to the active area of the filtered photodiodes. These dimensions yielded an angle of view of 2.56 degrees per sensor, approximately five times the angular diameter of the sun, but within aperture ranges reported for other low-cost sun photometers (Mims, 2002). A narrow viewing angle was required to mitigate errors caused by forward scattered sunlight 20 entering the field of view of the detector (Torres et al., 2013). The housing also included a sealed inlet and outlet for flow through the PMS5003 sensor. Two sockets with 1/4 - 20 Unified National Coarse threads allowed the AMOD to be mounted to standard camera tripods. The housing was weather-resistant when mounted in its intended orientation—, with the PM_{2.5} inlet facing the ground and the AOD apertures pointed toward the sun (Figure 2). An O-ring seal prevented leakage through the seam of the housing halves and float-glass windows sealed with foam adhesive protected the optical apertures.

25 The internal AMOD battery was a 3.6 V, 20.1 Ah custom battery pack comprised of six 18650 lithium ion cells (Panasonic NCR18650B, Kadoma, Japan). The battery was charged via a barrel plug port on the side of the housing. This plug accepted power from a wall charger, external battery, or solar panel (Voltaic[®] 3.5W) and was watertight when the solar panel cable was attached to the barrel port. The removable solar panel was mounted to the exterior housing using magnets adhered 30 to opposing surfaces on the panel and AMOD housing. Photographs of the external hardware in front and isometric orientations are provided in Figure 2.

The dimensions of the AMOD were 9.0 cm W x 14.1 cm H x 6.7 cm L and the weight was 0.64 kg. The total cost of goods of the AMOD was less than \$1,100 (Table S1). This tabulation was based on a production run of 24 units. The average assembly time for a single AMOD was estimated at two hours, which translated to a cost of \$50 at a rate of \$25 per hour.

2.2 Calibration Procedure

One AMOD master unit was calibrated relative to a Cimel CE318 at the DigitalGlobe AERONET site in Longmont, Colorado (Holben et al., 1998). AERONET instruments are calibrated using the Langley plot technique at Mauna Loa observatory—or relative to other AERONET instruments that have been so calibrated—to AOD uncertainties between 0.002 and 0.005 (Eck et al., 1999). The master AMOD ~~calibration consisted of~~ was calibrated relative to the Cimel CE318 by taking 5 co-located and concurrent measurements ~~taken~~ over the course of two to four hours. The extraterrestrial constant (V_0) was determined for each individual measurement by solving Eq. (2) using the AERONET value for AOD. The extraterrestrial constant for the master AMOD unit was then determined by averaging the extraterrestrial constant calculated from each individual measurement. The extraterrestrial constants of all other AMOD units were derived relative to the AMOD master 10 unit by taking a series of simultaneous measurements under variable illumination (Boersma and de Vroom, 2006). The extraterrestrial constant for all other units, $V_{0,i}$, was determined as follows (Boersma and de Vroom, 2006):

$$V_{0,i} = V_{0,master} \cdot \rho_i \quad (5)$$

where $V_{0,master}$ is the extraterrestrial constant of the master unit and ρ_i is the average ratio of photodiode voltage readings from uncalibrated unit i to the master unit. We recommend updating the calibration constants of AMOD instruments on a six-month basis to account for changes in optical properties of the optical interference filters and photodiodes. 15

2.3 AOD Calculation Algorithm

We developed AOD calculation firmware using an online, open-source platform (mbedTM; ARM[®] Ltd., Cambridge, UK), which was executed by the on-board microcontroller (STMicroelectronics STM32L152RE, Geneva, Switzerland). Prior to applying Eq. (2) to calculate AOD, the Earth-Sun distance (R), the relative optical air mass factor (m), and the Rayleigh 20 optical depth (τ_R) were determined in accordance with the measurement location, time, pressure, and temperature. The National Renewable Energy Laboratory (NREL) published a solar position algorithm to calculate azimuth, elevation and zenith angles at uncertainties equal to ± 0.0003 as a function of location, time and for years between 2000 and 6000 (Reda et al., 2008). This algorithm was implemented as a C++ microcontroller code to automate solar calculations for the AMOD. The Earth-Sun distance was calculated directly by the solar position algorithm.

25 The relative optical air mass factor was calculated in terms of the solar zenith angle, θ , as follows (Young, 1994):

$$m = \frac{1.002432 \cdot \cos^2(\theta) + 0.148386 \cdot \cos(\theta) + 0.0096467}{\cos^3(\theta) + 0.149864 \cdot \cos^2(\theta) + 0.0102963 \cdot \cos(\theta) + 0.000303978} \quad (6)$$

The contributions of Rayleigh scattering and ozone absorption to total optical depth are often substantial and must be subtracted from the total optical depth for accurate AOD measurements (Bodhaine et al., 1999). Rayleigh optical depth is inversely proportional to the fourth power of wavelength, which made accurate quantification especially important for the 440 30 nm and 520 nm channels on the AMOD. Rayleigh optical depth was calculated based on wavelength and ambient pressure measured by an on-board pressure sensor (Bosch Sensortec BMP 280, Kusterdingen, Germany) (Bodhaine et al., 1999). The AMOD's 520 nm and 680 nm channels were within the Chappuis ozone absorption band (450 nm – 850 nm). An empirical

model was used to estimate ozone concentrations in Dobson Units (DU)—based on the location and time of the measurement (Van Heuklon, 1979)—which were then used to determine the ozone optical depth (Koontz et al., 2013).

Finally, Eq. (2) was applied to determine the total optical depth using sensor inputs; the extraterrestrial constant; and the calculated Earth-Sun distance, relative optical air mass factor, Rayleigh optical depth, and ozone absorption optical depth.

5 AOD, temperature, pressure, relative humidity, time, ~~location~~, and ~~battery status were~~location were then stored on an accessible MicroSD card (Molex 5031821852, Lisle, IL, USA).

2.4 User Operation and Measurement Procedure

We designed the AMOD to be operated by individuals without a background in aerosol sampling but with an interest in air pollution and citizen science. Care was taken to minimize the complexity of the measurement process. A smartphone application guided the user through a single measurement in a series of steps (Figure S3). Items needed to complete a measurement included an AMOD unit, a filter cartridge loaded with a pre-weighed air-sampling filter, a smartphone (iOS or

10 Android enabled) with the device application (“CEAMS”; available on the Apple App Store and Google Play) downloaded, and a commercial tripod or alternative mount. Prior to initiating a measurement, the operator manually loaded the filter cartridge into position and aligned the AOD sensors with the sun. The alignment process was aided by an integrated pinhole and target apparatus, which was geometrically aligned with the filtered photodiodes (Figures 1, 2). Once the AMOD was

15 aligned, the operator initiated a sample with the smartphone application. The AMOD then recorded an instantaneous AOD measurement and began sampling air onto the filter under active control of ~~mass~~the sample flow rate at 2 L min⁻¹. The AMOD also began recording real-time PM_{2.5} levels reported by the PMS5003. Air sampling continued for 48.25 hours before the

20 AMOD automatically shut off. The AMOD maintained a fixed orientation on a tripod for the entire sampling duration—barring any unintended movements. The AMOD sampled AOD three times over the 48.25-hr sampling period: immediately after the sample started, 24 hours into the sample, and 48 hours into the sample (i.e., at each solar overpass). To partially mitigate errors caused by day-to-day changes in the Sun’s position, the AMOD began measuring AOD 15 minutes prior to the 24-hour mark and logged AOD values every 30 seconds until 15 minutes after the 24-hour mark. The operator was able to use this 30-minute window to correct the AMOD’s orientation if unintended movements had taken place since the start of the sample. The lowest

25 AOD values—which corresponded with the highest photodiode signal—signals, from the 30 minute measurement window at 24-hours and 48-hours were taken as the second and third AOD measurements. Upon completion of the sample, the operator downloaded data from the AMOD using the smartphone application and transferred the data to a host server.

2.5 Co-location Validation Studies

AMOD AOD measurements were validated in a series of co-location studies using AERONET CE318 monitors as the reference method (Holben et al., 1998). CE318 monitors used in the co-location studies had a 1.2° full angle field of view and measured AOD at eight wavelengths: 340 nm, 380 nm, 440 nm, 500 nm, 675 nm, 870 nm, 1020 nm, and 1640 nm (Holben et al., 1998). The CE318 monitors used stepping motors and closed loop control to locate and track the sun and reported

measurements every 3-15 minutes when solar alignment was achieved (Holben et al., 1998). AERONET monitors were available at two sites along the Colorado Front Range: NEON-CVALLA (N 40°09'39", W 105°10'01") and Digital Globe (N 40°08'20", W 105°08'13"). Device master calibrations were conducted at the Digital Globe site and device validation tests were conducted at NEON-CVALLA. Co-location tests took place on three separate days using seven different AMOD units: 5 one calibrated directly relative to AERONET at the Digital Globe site, and six calibrated via the transfer calibration method (Eq. 5). Between two and four calibrated AMOD units were randomly selected on each testing day and deployed within 50 m of the AERONET monitor. A total of seven AMOD instruments were used in co location studies. Four-wavelength AMOD AOD measurements were taken at five-minute intervals over the course of one to four hours on each measurement day. AMOD data were then compared with Level 1.0 AOD data published in the online AERONET database (Holben et al., 1998). AMOD 10 measurements concurrent within 2 minutes of an AERONET measurement were included in the comparison data set for the wavelength in question. The 500 nm and 675 nm AOD values from the AERONET instruments were adjusted—using Eq. (4) and Ångström coefficients from the AERONET data set—to match the 520 nm and 680 nm channels on the AMOD, respectively. The 440 nm and 870 nm channels required no adjustment because the AMOD and the AERONET monitors both measure at those wavelengths.

15 Time-integrated PM_{2.5} mass concentrations measured using the AMOD filter samples were validated in a series of 48-hr co-location tests conducted with FEM monitors. AMOD units were loaded with 37 mm PTFE filters (MTL PT37P-PF03, Minneapolis, MN USA). The FEM consisted of an EPA-certified Louvered Inlet (PM10 – Mesa Labs SSI2.5, Lakewood, CO USA) with an inline PM_{2.5} cyclone (URG Corp 2161, Chapel Hill, NC USA) operating at 16.7 L_{min}⁻¹. The PM_{2.5} sample was collected on a 47 mm PTFE filter (Tisch Scientific SF18040, North Bend, OH USA). Airflow through the inlet, cyclone, and 20 filter cartridge was maintained by a pump (Gast 86R142-P001B-N270X, Benton Harbor, MI USA) and metered using a mass-flow controller (Alicat MCRW-20SLPM-D/5M, Tucson, AZ USA). Co-location tests occurred in multiple locations—including downtown Fort Collins, the Colorado State University main campus, and at several personal residences across the city—over a 10-week period. We constructed a custom mount to support the FEM monitors and hold AMOD samplers at 40 cm from the FEM inlet (Figure S4).

25 The PM_{2.5} mass concentrations measured using the PMS5003 included in the AMOD were evaluated against a co-located light-scattering FEM monitor (EDM 180, GRIMM EDM 180, Ainring, Germany) at the Colorado State University main campus (EPA monitoring site 08-069-0009). Light The GRIMM utilized a 660 nm diode laser cell couple with a light detector to measure particle concentrations based on light scattering. Flow through the GRIMM was maintained at 1.2 L min⁻¹. PM_{2.5} readings from the AMOD PMS5003 were corrected *post hoc*, relative to the AMOD filter, by multiplying each light-scattering reading by a scaling factor equal to the ratio of the filter measurement to the 48-hr average of the PMS5003. The 30 PMS5003 outputs uncorrected PM_{2.5} concentrations as well as PM_{2.5} concentrations with a proprietary correction factor for use under atmospheric conditions. We used the corrected data output by the PMS5003 for our analyses. Hourly averages of the corrected readings were then calculated for comparison to the hourly concentrations reported by the GRIMM EDM 180.

3. Results and Discussion

3.1 AOD Sensor Evaluation

Close agreement was observed between the AMOD and AERONET monitors for AOD. A comparison plot for all wavelengths and all AERONET co-location testing data is provided in Figure 3 (n = 130 paired measurements for each wavelength). The mean absolute error between the AMOD and AERONET instruments was 0.0079 AOD units (across all wavelengths), yielding a mean relative error of 10%. These deviations were nearly within the published uncertainties of the AERONET monitors (0.002 – 0.005) (Eck et al., 1999). The mean AOD difference was 0.00063 with 95% confidence upper and lower limits of agreement of 0.026 and -0.024, respectively (Bland and Altman, 1986). A Bland-Altman plot illustrating the mean difference and limits of agreement is provided in Figure S5. The mean difference results indicated a low systematic bias between the two instruments in AOD units. The single set of outlier points shown in Figure 3 was most indicative of a misalignment error because: 1) the error relative to AERONET was at least 3× the error of all other measurements from the same AMOD unit; 2) measurements taken at the same time and location with different AMOD units exhibited lower error; and 3) the AOD was over-predicted by the AMOD, which is consistent with lower photodiode signal from misalignment. Agreement between AMOD units was comparable to the agreement between AMOD units and AERONET monitors. The average coefficient of variation between AMOD measurements, expressed as a percentage, was 9.0%. We observed negligible performance differences between a master AMOD unit calibrated directly against AERONET instruments and those calibrated via transfer calibrations (Eq. 5). The average difference between units calibrated via the transfer calibration and the master unit was 0.006 AOD units.

Our evaluation was limited to relatively low AOD values due to the low aerosol concentrations at regional AERONET stations in fall 2017. We do not view this limitation as consequential because the linear dynamic range of the photodetectors used in the AMOD includes AOD values from 0-5 AOD units (specific voltages associated with AOD values are wavelength and calibration dependent). We plan to expand our performance evaluation to a broader range of environmental conditions in future work. Thin cirrus cloud cover on some days likely yielded the highest AOD values; while this was not strictly “aerosol” optical depth, it allowed for validation across a greater AOD range against the non-cloud-filtered Level 1.0 AERONET data. Compared with AERONET monitors, the main advantages of the AMOD are its low cost and portability. The AMOD (including light-scattering and integrated PM_{2.5} monitoring) has a cost of goods <40× lower than the purchase price of an AERONET CE318 monitor. The cost of goods—particularly circuit boards and mechanical components—would be reduced at higher quantities. Reference-grade CE318 monitors are advantageous with respect to measurement automation (e.g., sun tracking allows for many measurements throughout the day), the number of AOD wavelengths (nine for the standard model), and the potential for additional sky radiation measurements beyond AOD (Holben et al., 1998).

AERONET co-location results indicate the AMOD can be used to measure AOD with high accuracy when measurements are initiated and overseen by an operator; however, it remains difficult to assess the reliability of unsupervised measurements taken at 24 and 48-hour intervals after the original measurement. Wind and other disturbances can cause slight

misalignment to occur between the first and second measurements. Any software adjustments made to compensate for the day-to-day variation in the sun's path assume stability of the AMOD throughout the sampling period. The proportions of the AOD apertures permit angular deviations from direct sunlight up to approximately 0.5° for acceptable measurements. In Colorado, for example, the average day-to-day variation—for airmass values less than five—in the solar zenith and azimuth angles is 5 0.2°. Based on those day-to-day variations, the AMOD is most sensitive alignment disturbances for measurements taken at the 48-hour mark. An accelerometer reports the angular pitch of the AMOD relative to horizontal on a 30-second basis. We used those data to determine if the AMOD underwent large angular changes (e.g. >2°) relative to the horizontal plane during sample collection. Wind and other disturbances can cause slight misalignment to occur between the first and second measurements 10 that may not be detectable by the accelerometer. To help catch these events, a quadrant-photodiode-based solar-alignment sensor, mounted parallel to the AOD sensors, could be added to the AMOD to measure solar incidence angle for deviations smaller than 5° at a precision of 0.1°. The sensor would measure solar alignment based on differential signals between elements 15 of a quadrant photodiode array. Without automated self-correction or operator intervention, misalignment manifests itself with erroneously high AOD measures, which are difficult to discriminate from similar to cloud-contaminated measurements. Manual screening requires operator attention, which cannot be expected for a 48+ hour sampling period. Automated cloud screening could benefit from active solar tracking and relatively high frequency measurements (Smirnov et al., 2000).; however, 20 erroneously high AOD measures, due to either misalignment or cloud contamination, can be identified and eliminated using an automated data screening algorithm.

The development of a low-cost solar tracking mount is also the subject of ongoing work. Active tracking would eliminate the need for algorithmic adjustments to account for daily solar position, enable measurement of daily AOD trends, 20 increase solar power input, and enable robust cloud-screening algorithms. Closed-loop solar tracking will be facilitated by the quadrant diode solar-alignment sensor included in Figure 1. The sensor measures solar alignment based on differential signals between elements of a quadrant photodiode array. Sensor-geometry specific calibration factors enable accurate computation of two-dimensional incidence angles. Incidence angle information will be used in conjunction with a closed-loop motor control algorithm to locate and track the Sun.

AMOD measurements are amenable to re-analysis using ozone data from outside models or retrievals (Wargan et al., 25 2017). Re-analysis may be used to compensate for NO₂ absorption in the 440 nm and 520 nm channels, which is unaccounted for in standard AMOD measurements. We plan to improve ozone compensation calculations as part of the second generation AMOD design. Karavana-Papadimou et al. (2013) modified the model (Van Heuklon, 1979) parameters used in the AMOD algorithm using updated ozone measurements for select European cities (Karavana-Papadimou et al., 2013). The updated 30 model achieved improved accuracy for European ozone predictions (Karavana-Papadimou et al., 2013). We plan to leverage ozone retrievals across the U.S. to improve the model presently implemented by the AMOD. This approach can be extended into other regions as the need arises.

3.2 Gravimetric PM_{2.5} Sampler Evaluation

Relatively good agreement was found between AMOD gravimetric PM_{2.5} and FEM samplers in the co-location study (see Figure 4) (Noble et al., 2001). The Pearson correlation between 39 co-located AMOD and FEM measurements was 0.93.

The Pearson correlation between 39 co-located AMOD and FEM measurements was 0.93. The mean absolute error was 0.83

5 $\mu\text{g m}^{-3}$, corresponding to a mean relative error of 8% between instruments. The mean difference was $-0.0037 \mu\text{g m}^{-3}$ with 95% confidence upper and lower limits of agreement of 1.84 and $-1.85 \mu\text{g m}^{-3}$ respectively (Bland and Altman, 1986). A Bland-Altman plot indicated a low systematic bias between the two instruments as a function of PM_{2.5} concentration (Figure S6). These results were consistent with the agreement observed in previous work between PM_{2.5} mass concentrations measured using UPAS gravimetric samples and other accepted gravimetric sampling techniques (Arku et al., 2018; Kelleher et al., 2018; 10 Pillarisetti et al., 2019; Volckens et al., 2017). These results are encouraging given the low 48-hour average PM_{2.5} concentrations in Fort Collins during this period (ranging from 3.9 to $12.4 \mu\text{g m}^{-3}$).

15 Agreement between AMOD units was comparable to the agreement between AMOD units and FEM monitors. The average coefficient of variation between AMOD measurements taken concurrently with different units, expressed as a percentage, was 6.8%. The relative standard deviation for AMOD gravimetric PM_{2.5} measurements collected using duplicate samplers at the same location was 4.9%.

20 The performance of the AMOD PM_{2.5} sampler was promising in the context of its low cost and compact, portable form factor relative to the FEM. The AMOD cost of goods was less than the purchase price of the FEM used in the co-location studies by a factor of 12. The AMOD was 97% lighter and more compact than the FEM when both were in their stowed configuration. Size comparisons when deployed depend on the apparatus used to mount the AMOD (e.g., camera tripod). The evaluation summarized in Figure 4 was limited to relatively clean conditions in Colorado. In previous works, we have evaluated cyclone performance at concentrations exceeding 20 from 15 $\mu\text{g m}^{-3}$ to 40 $\mu\text{g m}^{-3}$ and observed similar agreement with FEM monitors (Kelleher et al., 2018). (Kelleher et al., 2018). Further, the UPAS technology (the gravimetric sampling technology with which the AMOD was developed) has been evaluated against reference monitors by several groups at concentrations approaching 1000 $\mu\text{g m}^{-3}$ and in over 10 different countries with similar results (Arku et al., 2018; Pillarisetti et al., 2019).

25 3.3 Light-Scattering PM_{2.5} Sensor Evaluation

Preliminary co-location results for the AMOD light-scattering sensor indicated relatively good agreement with a GRIMM FEM light-scattering sensor, albeit with an apparent directional bias. A box plot of paired average vs. paired difference PM_{2.5} concentration is provided in Figure 5. Measurement pairs consist of temporally and spatially coincident, hourly average AMOD and FEM PM_{2.5} measurements. Reported AMOD measurements are filter-corrected. Concentrations 30 reported by the FEM ranged from 0 to $17 \mu\text{g m}^{-3}$. After normalizing the time-resolved AMOD measurements to the filter, the mean absolute error was $1.98 \mu\text{g m}^{-3}$. The mean difference was $0.04 \mu\text{g m}^{-3}$ with 95% confidence upper and lower limits of agreement of 5.02 and $-4.95 \mu\text{g m}^{-3}$, respectively (Bland and Altman, 1986). For pair-averaged PM_{2.5} concentrations less than

10 $\mu\text{g m}^{-3}$, AMOD measurements were generally low relative to FEM measurements. For pair-averaged $\text{PM}_{2.5}$ concentrations greater than 10 $\mu\text{g m}^{-3}$, AMOD measurements were generally high relative to FEM measurements. This trend held for both corrected and uncorrected AMOD light-scattering sensor measurements (Figure S7).

One limitation associated with the FEM and the PMS5003 is the low digital resolution. Both monitors report integer values (PMS5003 before filter normalization), which can magnify or obscure relative errors at low concentrations. Readings of 0 $\mu\text{g m}^{-3}$ are especially problematic because they cannot be corrected to the filter via scaling factor multiplication. This leaves zero readings uncorrected and tends to magnify the scaling of non-zero readings (Figure 5).

The AMOD light-scattering sensor represents cost savings over reference-quality light-scattering monitors and performance improvements over other low-cost sensors. The cost of goods of the AMOD is 20 \times less than the purchase prices of two reference quality monitors: the ThermoFisher Tapered Element Oscillating Microbalance (TEOMTM) and the GRIMM monitor used in the co-location studies. Filter correction and weatherproof hardware integration may increase the accuracy and durability of the AMOD light-scattering measurement system compared with stand-alone low-cost sensors.

3.4 Wireless Capability

Smartphone connectivity and control is an advantage of the AMOD. The custom AMOD smartphone application serves as a wireless control platform, condensed user manual, and data transfer tool. Wireless control allows the user to start the sampler without the risk of altering an established alignment. Systematic instructions reduce the potential for operator error and omission. Wireless data transfer is less labor intensive than hardware alternatives (e.g., SDTM card) and can be directly interfaced with a web server via the smartphone Wi-Fi. The present BluetoothTM smartphone application cannot connect to the AMOD while running, cannot display run data in the app, and downloads data at slow speeds (often in excess of five minutes for a full 48.25-hr dataset). Expanding the web connectivity of the AMOD to include real-time data transfer and visualization using the Wi-Fi chip is the subject of ongoing work. Basic data transfer and real-time visualization capabilities have been developed for the AMOD using a free Internet of Things (IoT) service (ThingSpeakTM) and the ESP8266 Wi-Fi chip. Further development could enable faster data transfer and immediate feedback for participants in AMOD deployments. These capabilities could bolster the scientific potential of AMOD data, provide an interface with other web-connected devices, and facilitate operator engagement.

3.5 Potential Sampler Network

The unique combination of AOD, gravimetric filter $\text{PM}_{2.5}$, and real-time $\text{PM}_{2.5}$ sampling on a compact, user-friendly, and relatively low-cost platform, make the AMOD amenable to large-scale deployment in spatially dense sampling networks. Given these characteristics, the AMOD can be deployed in large numbers, by either trained or citizen scientists, to collect spatially dense AOD and $\text{PM}_{2.5}$ data sets. These data sets, which can be used to gain a better understanding of spatial and temporal variations in the relationship between AOD and $\text{PM}_{2.5}$ concentration, have the potential to improve and expand the use of satellite AOD-derived estimates of ground-level $\text{PM}_{2.5}$ concentrations.

4 Conclusions

The AMOD is a lightweight and compact alternative to the instruments typically used to sample AOD and PM_{2.5}. The AMOD represents a substantial cost saving compared with alternative AOD and PM_{2.5} mass concentration sampling equipment. In field testing, the AMOD exhibit agreement within 10% when compared with AOD and PM_{2.5} reference instruments. The AMOD has been validated only in a relatively clean air in Colorado in fall and wintertime; more validation in other environments of varying pollution/weather patterns is needed. The small size, durability, increased sampling capabilities and relatively low cost of the AMOD make it a viable option for large scale and spatially dense deployments. Such data sets have the potential to facilitate the calibration and validation of satellite-based sensors as they progress toward higher spatial resolution measurement capabilities.

10 Acknowledgements

This work was supported by the National Aeronautics and Space Administration under Agreement No. NNX17AF94A and the State of Colorado Office of Economic Development and Information Technology. The authors wish to thank John Mehaffy, Scott Kelleher, David Brooks, Marilee Long, Lizette van Zyl, Todd Hochwitz (Zebulon Solutions LLC, Longmont, CO USA), Josh Smith, and Caroline Wendt for their contributions to this work. The authors also thank 15 Michele Kuester of Digital Globe and Janae Csavina of NEON for their help securing AERONET co-location sites.

References

Ångström, A.: On the Atmospheric Transmission of Sun Radiation and on Dust in the Air, Geogr. Ann., 11, 156, doi:10.2307/519399, 1929.

20 AQ-SPEC: PurpleAir PA II, [online] Available from: <http://www.aqmd.gov/aq-spec/product/purpleair-pa-ii> (Accessed 10 May 2018), n.d.

Arku, R. E., Birch, A., Shupler, M., Yusuf, S., Hystad, P. and Brauer, M.: Characterizing exposure to household air pollution within the Prospective Urban Rural Epidemiology (PURE) study, Environ. Int., 114(January), 307–317, doi:10.1016/j.envint.2018.02.033, 2018.

Bland, M. J. and Altman, D.: Statistical Methods for Assessing Agreement Between Two Methods of Clinical Measurement, 25 Lancet, 327(8476), 307–310, doi:10.1016/S0140-6736(86)90837-8, 1986.

Bodhaine, B. A., Wood, N. B., Dutton, E. G. and Slusser, J. R.: On Rayleigh optical depth calculations, J. Atmos. Ocean. Technol., 16(11 PART 2), 1854–1861, doi:10.1175/1520-0426(1999)016<1854:ORODC>2.0.CO;2, 1999.

Boersma, K. F. and de Vroom, J. P.: Validation of MODIS aerosol observations over the Netherlands with GLOBE student measurements, J. Geophys. Res. Atmos., 111(20), 1–14, doi:10.1029/2006JD007172, 2006.

30 Brauer, M., Freedman, G., Frostad, J., van Donkelaar, A., Martin, R. V., Dentener, F., Dingenen, R. van, Estep, K., Amini, H.,

Apte, J. S., Balakrishnan, K., Barregard, L., Broday, D., Feigin, V., Ghosh, S., Hopke, P. K., Knibbs, L. D., Kokubo, Y., Liu, Y., Ma, S., Morawska, L., Sangrador, J. L. T., Shaddick, G., Anderson, H. R., Vos, T., Forouzanfar, M. H., Burnett, R. T. and Cohen, A.: Ambient Air Pollution Exposure Estimation for the Global Burden of Disease 2013, *Environ. Sci. Technol.*, 50(1), 79–88, doi:10.1021/acs.est.5b03709, 2016.

5 Brooks, D. R., F. M. M.: Development of an inexpensive handheld LED-based Sun photometer for the GLOBE program, *J. Geophys. Res.*, 106(16), 4733–4740, doi:10.1029/2000JD900545, 2001.

Bulot, F. M. J., Johnston, S. J., Basford, P. J., Easton, N. H. C., Apetroaie-cristea, M., Foster, G. L., Morris, A. K. R. and Cox, S. J.: Long-term field comparison of multiple low-cost particulate matter sensors in an outdoor urban environment, *Sci. Rep.*, (April), 1–13, doi:10.1038/s41598-019-43716-3, 2019.

10 van Donkelaar, A., Martin, R. V. and Park, R. J.: Estimating ground-level PM2.5 using aerosol optical depth determined from satellite remote sensing, *J. Geophys. Res. Atmos.*, 111(21), 1–10, doi:10.1029/2005JD006996, 2006.

van Donkelaar, A., Martin, R. V., Brauer, M., Kahn, R., Levy, R., Verduzco, C. and Villeneuve, P. J.: Global estimates of ambient fine particulate matter concentrations from satellite-based aerosol optical depth: Development and application, *Environ. Health Perspect.*, 118(6), 847–855, doi:10.1289/ehp.0901623, 2010.

15 van Donkelaar, A., Martin, R. V., Spurr, R. J. D., Drury, E., Remer, L. A., Levy, R. C. and Wang, J.: Optimal estimation for global ground-level fine particulate matter concentrations, *J. Geophys. Res. Atmos.*, 118(11), 5621–5636, doi:10.1002/jgrd.50479, 2013.

Eck, T. F., Holben, B. N., Reid, J. S., Dubovik, O., Smirnov, A., O'Neill, N. T., Slutsker, I. and Kinne, S.: Wavelength dependence of the optical depth of biomass burning, urban, and desert dust aerosols, *J. Geophys. Res. Atmos.*, 104(D24), 20 31333–31349, doi:10.1029/1999JD900923, 1999.

Forouzanfar, M. H., Afshin, A., Alexander, L. T., Biryukov, S., Brauer, M., Cercy, K., Charlson, F. J., Cohen, A. J., Dandona, L., Estep, K., Ferrari, A. J., Frostad, J. J., Fullman, N., Godwin, W. W., Griswold, M., Hay, S. I., Kyu, H. H., Larson, H. J., Lim, S. S., Liu, P. Y., Lopez, A. D., Lozano, R., Marczak, L., Mokdad, A. H., Moradi-Lakeh, M., Naghavi, M., Reitsma, M. B., Roth, G. A., Sur, P. J., Vos, T., Wagner, J. A., Wang, H., Zhao, Y., Zhou, M., Barber, R. M., Bell, B., Blore, J. D., Casey, 25 D. C., Coates, M. M., Cooperrider, K., Cornaby, L., Dicker, D., Erskine, H. E., Fleming, T., Foreman, K., Gakidou, E., Haagsma, J. A., Johnson, C. O., Kemmer, L., Ku, T., Leung, J., Masiye, F., Millear, A., Mirarefin, M., Misganaw, A., Mullany, E., Mumford, J. E., Ng, M., Olsen, H., Rao, P., Reinig, N., Roman, Y., Sandar, L., Santomauro, D. F., Slepak, E. L., Sorensen, R. J. D., Thomas, B. A., Vollset, S. E., Whiteford, H. A., Zipkin, B., Murray, C. J. L., Mock, C. N., Anderson, B. O., Futran, N. D., Anderson, H. R., Bhutta, Z. A., Nisar, M. I., Akseer, N., Krueger, H., Gotay, C. C., Kissoon, N., Kopec, J. A., Pourmalek, 30 F., Burnett, R., Abajobir, A. A., Knibbs, L. D., Veerman, J. L., Laloo, R., Scott, J. G., Alam, N. K. M., Gouda, H. N., Guo, Y., McGrath, J. J., Charlson, F. J., Jeemon, P., Dandona, R., Goenka, S., Kumar, G. A., Gething, P. W., et al.: Global, regional, and national comparative risk assessment of 79 behavioural, environmental and occupational, and metabolic risks or clusters of risks, 1990–2015: a systematic analysis for the Global Burden of Disease Study 2015, *Lancet*, 388(10053), 1659–1724, doi:10.1016/S0140-6736(16)31679-8, 2016.

Guenter, J. and Tatum, J.: VCSEL Based Optical Sensors., 2002.

Van Heuklon, T. K.: Estimating atmospheric ozone for solar radiation models, *Sol. Energy*, 22(1), 63–68, doi:10.1016/0038-092X(79)90060-4, 1979.

Holben, B. N., Eck, T. F., Slutsker, I., Tanré, D., Buis, J. P., Setzer, A., Vermote, E., Reagan, J. A., Kaufman, Y. J., Nakajima, T., Lavenu, F., Jankowiak, I. and Smirnov, A.: AERONET—A Federated Instrument Network and Data Archive for Aerosol Characterization, *Remote Sens. Environ.*, 66(1), 1–16, doi:10.1016/S0034-4257(98)00031-5, 1998.

Karavana-Papadimou, K., Psiloglou, B. E., Lykoudis, S. and Kambezidis, H. D.: Model for estimating atmospheric ozone content over Europe for use in solar radiation algorithms, *Glob. Nest J.*, 15(2), 152–162, 2013.

Kelleher, S., Quinn, C., Miller-Lionberg, D. and Volckens, J.: A low-cost particulate matter (PM2.5) monitor for wildland fire smoke, *Atmos. Meas. Tech.*, 11(2), 1087–1097, doi:10.5194/amt-11-1087-2018, 2018.

~~Kelly, K. E., Whitaker, J., Petty, A., Widmer, C., Dybwad, A., Sleeth, D., Martin, R. and Butterfield, A.: Ambient and laboratory evaluation of a low cost particulate matter sensor, *Environ. Pollut.*, 221, 491–500, doi:10.1016/j.envpol.2016.12.039, 2017.~~

Koontz, A., Flynn, C., Hodges, G., Michalsky, J. and Barnard, J.: Aerosol Optical Depth Value-Added Product, US Dep. Energy, (March), 32, 2013.

Levy, R. C., Remer, L. a., Martins, J. V., Kaufman, Y. J., Plana-Fattori, a., Redemann, J. and Wenny, B.: Evaluation of the MODIS Aerosol Retrievals over Ocean and Land during CLAMS, *J. Atmos. Sci.*, 62, 974–992, doi:10.1175/JAS3391.1, 2005.

Levy Zamora, M., Xiong, F., Gentner, D., Kerkez, B., Kohrman-Glaser, J. and Koehler, K.: Field and Laboratory Evaluations of the Low-Cost Plantower Particulate Matter Sensor, *Environ. Sci. Technol.*, 53(2), 838–849, doi:10.1021/acs.est.8b05174, 2019.

Lv, B., Hu, Y., Chang, H. H., Russell, A. G. and Bai, Y.: Improving the Accuracy of Daily PM_{2.5} Distributions Derived from the Fusion of Ground-Level Measurements with Aerosol Optical Depth Observations, a Case Study in North China, *Environ. Sci. Technol.*, 50(9), 4752–4759, doi:10.1021/acs.est.5b05940, 2016.

Mims, F. M.: Educational affairs: An International Haze-Monitoring Network for Students, *Bull. Am. Meteorol. Soc.*, 80(7), 1421–1431, 1999.

Mims, F. M.: An inexpensive and stable LED Sun photometer for measuring the water vapor column over South Texas from 1990 to 2001, *Geophys. Res. Lett.*, 29(13), 2–5, doi:10.1029/2002GL014776, 2002.

Mims III, F. M.: Sun photometer with light-emitting diodes as spectrally selective detectors, *Appl. Opt.*, 31(33), 6965–6967, 1992.

Murphy, D. M., Telg, H., Eck, T. F., Rodriguez, J., Stalin, S. E. and Bates, T. S.: A miniature scanning sun photometer for vertical profiles and mobile platforms, *Aerosol Sci. Technol.*, 50(1), 11–16, doi:10.1080/02786826.2015.1121200, 2016.

Nel, A.: Air Pollution – Related Illness: Effects of Particles, *Science* (80-), 308(5723), 804–806, doi:10.1126/science.1108752, 2005.

Noble, C. A., Vanderpool, R. W., Peters, T. M., Frank, F. M., Gemmill, D. B. and Wiener, R. W.: Federal Reference and

Equivalent Methods for Measuring Fine Particulate Matter Federal Reference and Equivalent Methods for Measuring Fine Particulate Matter, *Aerosol Sci. Technol.*, 34(5), 457–464, 2001.

O'Neill, N. T.: Spectral discrimination of coarse and fine mode optical depth, *J. Geophys. Res.*, 108(D17), 4559, doi:10.1029/2002JD002975, 2003.

5 Pillarisetti, A., Carter, E., Rajkumar, S., Young, B. N., Benka-Coker, M. L., Peel, J. L., Johnson, M. and Clark, M. L.: Measuring personal exposure to fine particulate matter (PM2.5) among rural Honduran women: A field evaluation of the Ultrasonic Personal Aerosol Sampler (UPAS), *Environ. Int.*, 123(September 2018), 50–53, doi:10.1016/j.envint.2018.11.014, 2019.

Pope, C. A. and Dockery, D. W.: Health effects of fine particulate air pollution: Lines that connect, *J. Air Waste Manag.*

10 Assoc., 56(6), 709–742, doi:10.1080/10473289.2006.10464485, 2006.

Reda, I., Andreas, A. and Nrel, A. A.: Solar Position Algorithm for Solar Radiation Applications (Revised), Nrel/Tp-560-34302, (January), 1–56, doi:10.1016/j.solener.2003.12.003, 2008.

Rollin, E. M.: An Introduction to the Use of Sun-photometry for the Atmospheric Correction of Airborne Sensor Data, , (Figure 1), 1–22, 2000.

15 Shaw, G. E.: Sun Photometry, *Bull. Am. Meteorol. Soc.*, 64(1), 4–10, doi:10.1175/1520-0477(1983)064<0004:SP>2.0.CO;2, 1983.

~~Smirnov, A., Holben, B. N., Eek, T. F., Dubovik, O. and Slutsker, I.: Cloud screening and quality control algorithms for the AERONET database, *Remote Sens. Environ.*, 73(3), 337–349, doi:10.1016/S0034-4257(00)00109-7, 2000.~~

Snider, G., Weagle, C. L., Martin, R. V., Van Donkelaar, A., Conrad, K., Cunningham, D., Gordon, C., Zwicker, M., Akoshile, C., Artaxo, P., Anh, N. X., Brook, J., Dong, J., Garland, R. M., Greenwald, R., Griffith, D., He, K., Holben, B. N., Kahn, R., Koren, I., Lagrosas, N., Lestari, P., Ma, Z., Vanderlei Martins, J., Quel, E. J., Rudich, Y., Salam, A., Tripathi, S. N., Yu, C., Zhang, Q., Zhang, Y., Brauer, M., Cohen, A., Gibson, M. D. and Liu, Y.: SPARTAN: A global network to evaluate and enhance satellite-based estimates of ground-level particulate matter for global health applications, *Atmos. Meas. Tech.*, 8(1), 505–521, doi:10.5194/amt-8-505-2015, 2015.

25 Torres, B., Toledano, C., Berjón, A., Fuertes, D., Molina, V., Gonzalez, R., Canini, M., Cachorro, V. E., Goloub, P., Podvin, T., Blarel, L., Dubovik, O., Bennouna, Y. and De Frutos, A. M.: Geoscientific Instrumentation Methods and Data Systems Measurements on pointing error and field of view of Cimel-318 Sun photometers in the scope of AERONET, *Atmos. Meas. Tech.*, 6, 2207–2220, doi:10.5194/amt-6-2207-2013, 2013.

US EPA: List of Designated Reference and Equivalent Methods., 2017.

30 Volckens, J., Quinn, C., Leith, D., Mehaffy, J., Henry, C. S. and Miller-Lionberg, D.: Development and evaluation of an ultrasonic personal aerosol sampler, *Indoor Air*, 27(2), 409–416, doi:10.1111/ina.12318, 2017.

Vroom, J. De and Amsterdam, V. U.: The Contribution of Dutch GLOBE Schools to Validation of Aerosol Measurements from Space, , (October), 2003.

Wargan, K., Labow, G., Frith, S., Pawson, S., Livesey, N. and Partyka, G.: Evaluation of the ozone fields in NASA's MERRA-

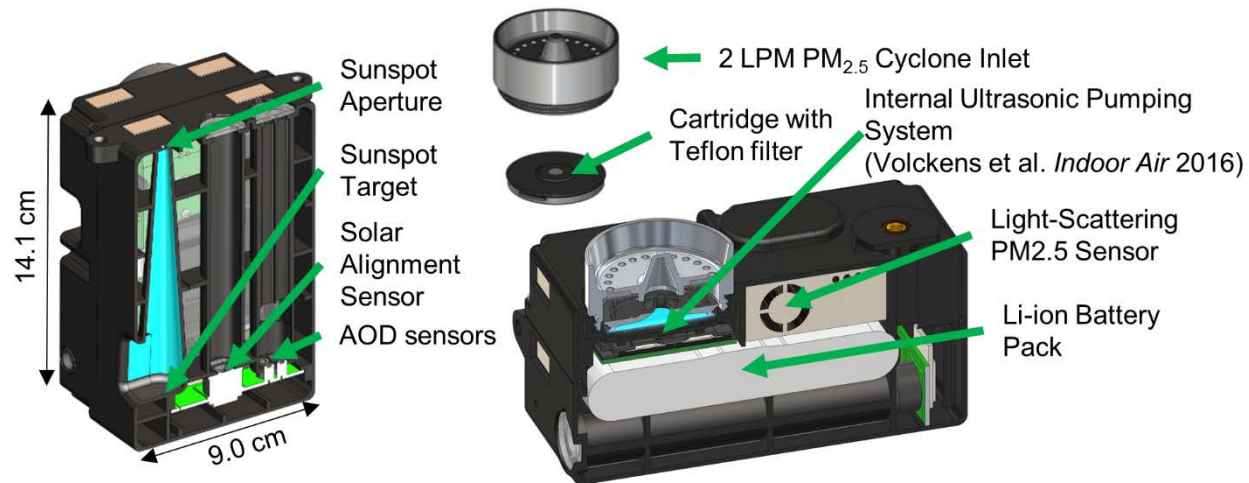
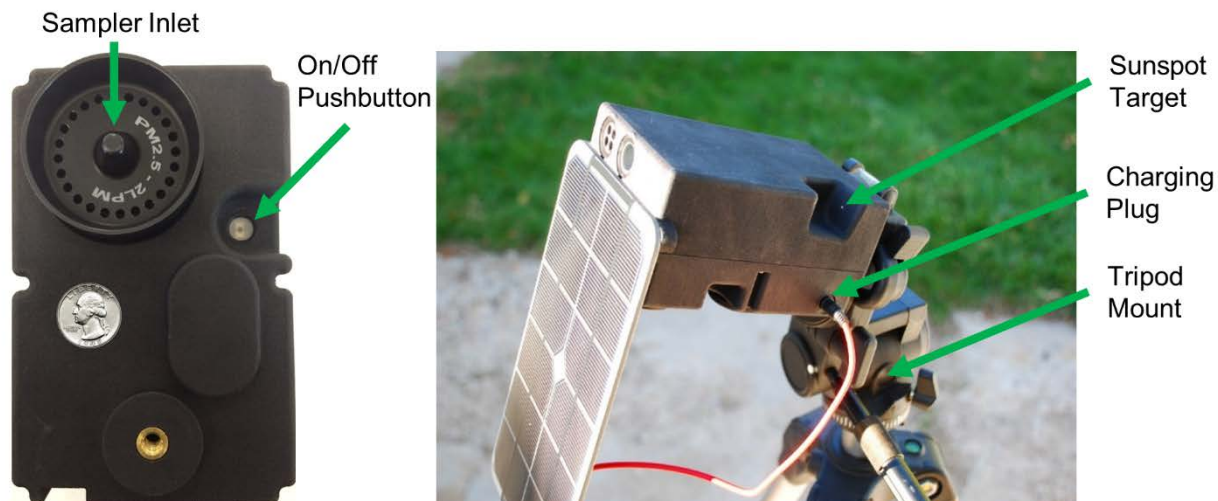


Figure 1: Computer-aided design rendering of key components of the AMOD including AOD and PM_{2.5} measurement systems, shown as cross-sectional cutaways.



10 Figure 2: Photographs highlighting AMOD external hardware.

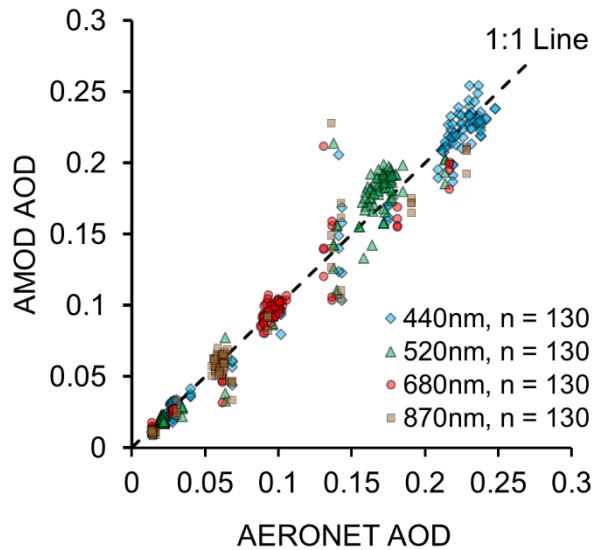
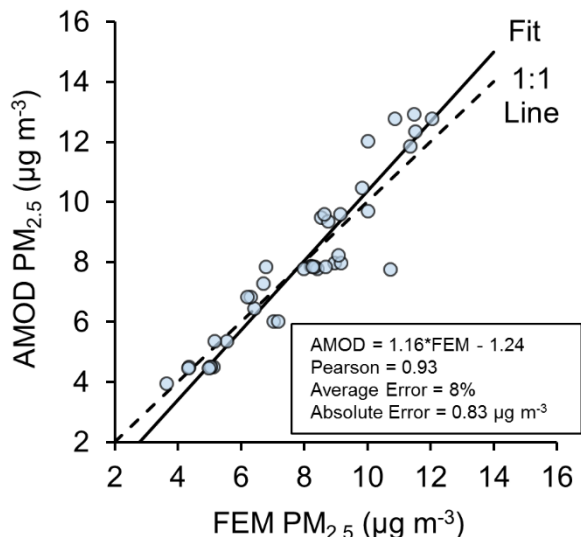


Figure 3: AERONET vs. AMOD AOD comparison plot. This plot includes all co-located measurements taken across all wavelengths between 3 September and 25 November of 2017.



5

Figure 4: FEM PM_{2.5} measurements vs. AMOD PM_{2.5} measurements in $\mu\text{g m}^{-3}$ (n = 39). Each data point represents a single 48-hr time-weighted average. All fit statistics were evaluated via Deming regression, assuming equal variance contributions from both measurement devices.

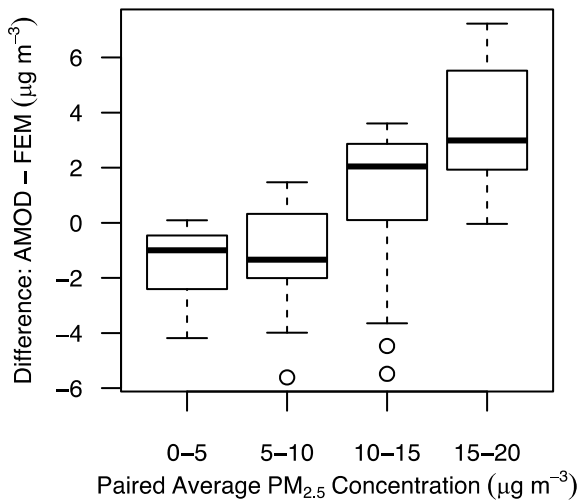


Figure 5: Binned paired average PM_{2.5} concentration vs. paired difference AMOD and FEM PM_{2.5} measurements. Measurement pairs ($n = 96$) consist of AMOD and FEM measurements that are temporally and spatially coincident. The four size bins (upper bound inclusive) are 0-5 $\mu\text{g m}^{-3}$ ($n = 30$), 5-10 $\mu\text{g m}^{-3}$ ($n = 24$), 10-15 $\mu\text{g m}^{-3}$ ($n = 30$), and 15-20 $\mu\text{g m}^{-3}$ ($n = 12$). All light-scattering

5 **AMOD measurements are include the proprietary PMS5003 atmospheric correction and are further** corrected to the corresponding AMOD filter measurement.